ISBN: 978-3-95450-261-5 ISSN: 2673-7000 doi: 10.18429/JACoW-NAPAC2025-THP052

MEASUREMENTS OF SINGLE-SHOT ATTOSECOND X-RAY PULSES AT HIGH REPETITION RATE*

V. Guo†, P. Franz, E. Isele, R. Robles, E. Thierstein, J. Wang
Stanford University, Stanford, CA, USA
K. Borne, M. Britton, D. Cesar, X. Li, M.F. Lin, R. Obaid, N. Sudar, J. Cryan, T. Driver, A. Marinelli
SLAC National Accelerator Laboratory, Menlo Park, CA, USA

Abstract

Electron dynamics in molecules occur on attosecond timescales and drive fundamental processes such as photosynthesis, catalysis, and chemical bond transformations. Understanding these phenomena requires tools with both high temporal resolution and the capability to probe molecular dynamics at high repetition rates. Here, we present the first single-shot measurements of attosecond soft X-ray pulses at the superconducting LCLS-II accelerator. Using an angle-resolving electron time-of-flight spectrometer, we perform angular streaking measurements with high energy and angular resolution, enabling a complete reconstruction of the spatial and temporal profiles of the pulses. These measurements showcase the attosecond science capabilities of LCLS-II at unprecedented repetition rates and provide the foundation for controlling and shaping X-ray pulses to study ultrafast dynamics in complex systems with precision.

INTRODUCTION

Electronic motions in molecular systems occur on sub-femtosecond time-scales. In order to resolve these dynamics, sub-femtosecond sources are needed. Previous experiments at LCLS have demonstrated attosecond capabilities at 120 Hz. This operation mode, named X-ray laser-enhanced attosecond pulse generation (XLEAP), can provide isolated attosecond pulses with tens of microjoules of energy, which is more than six orders of magnitude greater compared to common table-top high harmonic generation (HHG) sources [1, 2]. Here, we report the development of attosecond pulse generation to kHz repetition rates and a pulse reconstruction technique for full spectrotemporal characterizations.

METHODS

Data Collection

The X-ray pulse characterization is done via angular streaking measurements taken with a Multi-Resolution 'Cookiebox' (MRCO) detector, which consists of 16 time-of-flight (ToF) spectrometers forming a circular array in the plane perpendicular to the direction of X-ray propagation [3]. It is designed to be compatible with the ultimate 1 MHz repetition rate of LCLS-II, replacing the coaxial velocity mapping imaging spectrometer from previous LCLS pulse measurements, which can only operate at low repetition rates [4]. During data collection, x-rays ionize a sample gas, generating photoelectrons that are then streaked with an overlapped circularly polarized infrared laser. The spectrometer records hits from photoelectrons as digitized times of flight from the interaction point to the detectors.

Pulse Reconstruction

The X-ray pulse reconstruction is done using gradient descent optimization based on a basis representation of isolated attosecond pulses (IAPs) [5]. Since the spectral profiles of IAPs approximately have compact support, based on the Nyquist-Shannon sampling theorem, the electric field of an X-ray pulse can be completely determined by the reconstruction of points sampled above twice its bandwidth. The Whittaker-Shannon interpolation formula then allows the field to be represented by a decomposition onto a basis of orthogonal sinc functions,

$$E(t) = \sum_k E(t_k)\,\mathrm{sinc}(p(t - t_k)), \tag{1}$$

where p is the sampling frequency [6, 7].

The effect of streaking can be simulated for each basis function from analytically solving the time-dependent Schrodinger equation for the laser-atom interaction in the Strong-Field Approximation (SFA). Then, the probability distribution of photoelectrons associated with an IAP can be decomposed into

$$b(\vec{p}) = \sum_n c_n f_n(\vec{p}), \tag{2}$$

where $f_n(\vec{p})$ is the simulated streaking pattern of each basis function. The measured streaking pattern in experiment can then be described by

$$B(\vec{p}) = \sum_n \sum_m c_n^* c_m f_n^*(\vec{p}) f_m(\vec{p}), \tag{3}$$

and the basis coefficients c_n can be optimized to reconstruct the original X-ray electric field [5].

PRELIMINARY RESULTS

Simulation

To demonstrate the possibility of pulse reconstruction under experimental conditions and estimate the error in reconstructions, we first perform reconstructions on simulated attosecond pulses. Streaking traces are calculated from SFA simulations, and Poisson sampling noise is added to the sim-

* This work was supported by US Department of Energy contract nos. DE-AC02-76SF00515, the DOE-BES Accelerator and detector research program, and DOE-BES, Chemical Sciences, Geosciences, and Biosciences.
† vguo@slac.stanford.edu

ISBN: 978-3-95450-261-5 ISSN: 2673-7000 doi: 10.18429/JACoW-NAPAC2025-THP052

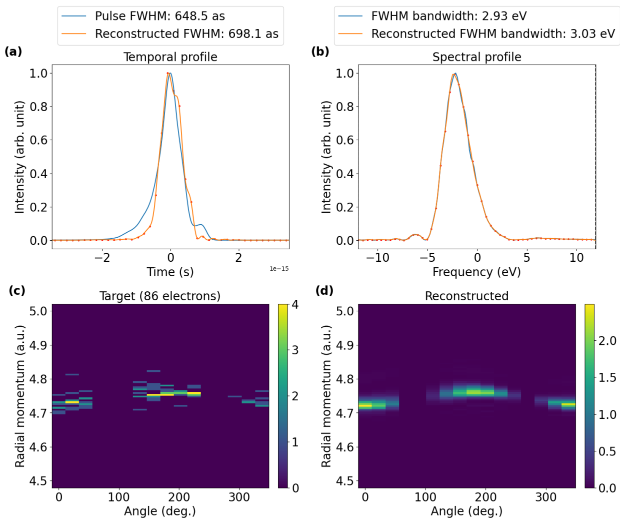

Figure 1: Single-shot reconstruction of a simulated attosecond pulse. (a) Temporal profiles of the simulated pulse and its reconstruction. (b) Spectral profiles of the simulated pulse and its reconstruction. (c) Simulated angular streaking trace with Poisson sampling noise. (d) Reconstructed angular streaking trace.

ulated electron distribution based on the measured collection efficiency of the MRCO. The spectral profile is used in the optimization as an initial guess, since recorded spectra are available in the experiment. The reconstruction algorithm performs minimization between the target streaking image and the reconstructed streaking image to optimize for the correct X-ray field. Figure 1 shows a single reconstruction of a simulated attosecond pulse. While the Poisson sampling noise from limited collection efficiency and low streaking amplitude limits the resolution of streaking features in the data, simulations show that the experimental conditions preserve sufficient information for pulse reconstructions.

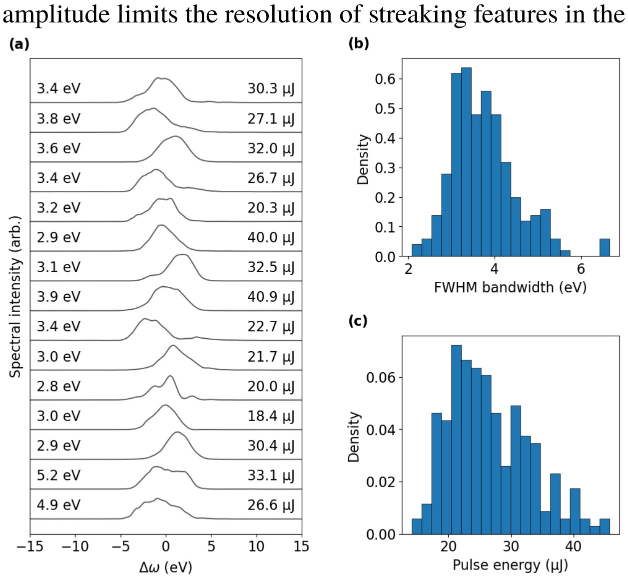

Figure 2: Characteristics of pulses generated in attosecond mode at high repetition rate at LCLS-II. (a) Example spectral profiles of 15 randomly selected shots. (b) Distribution of FWHM bandwidth. (c) Distribution of pulse energy.

Experimental Data

Using the XLEAP operation mode, we performed angular streaking measurements of soft X-ray pulses at 8 kHz at LCLS-II. Figure 2 shows some representative shots of spectral profiles as well as statistics on the spectral bandwidth and pulse energy. The mean FWHM bandwidth recorded is 3.8 eV, with an average pulse energy of 26.5 μJ. The recorded spectra show single-spike profiles, which suggest single-spike profiles in the time domain. The pulses also have sufficient bandwidth for sub-femtosecond pulse durations. For future work, recorded angular streaking measurements will be used to reconstruct the temporal profiles of these pulses.

CONCLUSION

Preliminary simulations suggest we can reconstruct sub-femtosecond pulses taken at high repetition rates using angular streaking measurements. Experimental data for pulse reconstruction has been taken at LCLS-II in the attosecond operation mode at 8 kHz. Future work will use the recorded angular streaking measurements to reconstruct the temporal profiles of the x-ray pulses.

ACKNOWLEDGEMENTS

Registration and lodging for NAPAC 2025 supported by the NAPAC 2025 student grant.

REFERENCES

[1] J. Duris *et al.*, “Tunable isolated attosecond X-ray pulses with gigawatt peak power from a free-electron laser”, *Nat. Photonics*, vol. 14, no. 1, pp. 30–36, Jan. 2020. doi:10.1038/s41566-019-0549-5

[2] P. Franz *et al.*, “Terawatt-scale attosecond X-ray pulses from a cascaded superradiant free-electron laser”, *Nat. Photonics*, May 2024. doi:10.1038/s41566-024-01427-w

[3] P. Walter *et al.*, “Multi-resolution electron spectrometer array for future free-electron laser experiments”, *J. Synchrotron Radiat.*, vol. 28, no. 5, pp. 1364–1376, Sep. 2021. doi:10.1107/S1600577521007700

[4] S. Li *et al.*, “A co-axial velocity map imaging spectrometer for electrons”, *AIP Adv.*, vol. 8, no. 11, p. 115308, Nov. 2018. doi:10.1063/1.5046192

[5] S. Li *et al.*, “Characterizing isolated attosecond pulses with angular streaking”, *Opt. Express*, vol. 26, no. 4, pp. 4531–4547, Feb. 2018. doi:10.1364/OE.26.004531

[6] CE. Shannon, “Communication in the presence of noise”, *Proceedings of the IRE*, vol. 37, no. 1, pp. 10–21, Jan. 1949. doi:10.1109/jrproc.1949.232969

[7] E. T. Whittaker, “XVIII.—on the functions which are represented by the expansions of the interpolation-theory”, *Proceedings of the Royal Society of Edinburgh*, vol. 35, pp. 181–194, 1915. doi:10.1017/S0370164600017806